Eur. Phys. J. D **4**, 353–364 (1998)

THE EUROPEAN PHYSICAL JOURNAL D

On charged mesoscopic metallic bubbles*

K. Pomorski[1,a] and K. Dietrich[2]

[1] Theoretical Physics Department, University MCS, Lublin, Poland
[2] Physik Department of the Technische Universität München, Garching, Germany

Received: 17 November 1997 / Revised: 28 May 1998 / Accepted: 20 July 1998

Abstract. We investigate the existence of stable charged metallic bubbles using the shell correction method. We find that for a given mesoscopic system of n atoms of a given metal and $q \ll n$ (positive) elementary charges, a metallic bubble turns out to have a lower total energy than a compact spherical cluster, whenever the charge number q is larger than a critical charge number q_c. For a magic number $(n-q)$ of free electrons, the spherical metallic bubble may become stable against fission.

PACS. 36.20.Kd Electronic structure and spectra – 31.10.+z Theory of electronic structure, electronic transitions, and chemical binding – 21.90.+f Other topics in nuclear structure – 21.60.Cs Shell model

1 Introduction

Neutral and charged metal clusters consisting of a few 100 to a few 1000 atoms possibly containing a limited number (≤ 10) of positive or negative surplus charges received considerable scientific interest since 1984. At that time, when studying the formation of tiny alkali clusters out of metal vapor, an enhanced production of clusters with certain atomic numbers (n = 8, 20, 40, 58, 92, *etc.*) was observed [1,2] and was correlated with the appearance of shell closures for the motion of the free electrons *i.e.* the conduction (valence) electrons in a spherically symmetric average potential for the itinerant electrons. A free electron feels an average potential which is produced by the background of positive ions, on the one hand, and by the other free electrons, on the other.

The most prominent peaks in the mass yield were shown to be due to shell closures in a spherically symmetric potential [3–8], whereas tinier details of the abundance curve were successfully related to secondary shell effects in axially symmetric deformed [9–11] and non-axially symmetric deformed [12] potentials.

The calculations are usually performed using the Strutinsky shell correction method [13] or the more involved self-consistent field approach [14,15].

A large amount of beautiful experimental work [16,17] has been performed since the discovery in 1984. The comparison between the experimental and theoretical work (see for instance Ref. [10]) is in general satisfactory. The greatest part of the work has hitherto been devoted to uncharged clusters. Experiments on charged metallic clusters were performed by Bréchignac *et al.* for Li_n^{+q} (n = number of atoms, q = number of elementary charge units) in reference [18] and for Sb_n^{+q} in reference [19]. It was found that in most cases singly charged clusters are stable, *i.e.* their dissociation is endothermic. Clusters with a positive charge $q > 1$ are observed if the number n of constituent atoms is larger than a critical number n_b^q which depends on the system considered. Decay by fission and by evaporation of neutral or charged fragments compete with each other, the decay by fission being delayed with respect to the decay by evaporation.

Theoretical studies of the decay were published by Garcias *et al.* [20] using a semi-empirical model for the fission of multiply charged metal clusters and by Gross *et al.* [21].

In all the theoretical studies of mesoscopic metallic clusters it was assumed that the ground state of the cluster corresponds either to a compact spherical or to a compact deformed shape.

As we show in this paper, for large enough charge q, the state of lowest energy of a charged metallic cluster may correspond to a spherical bubble. Within the liquid drop approximation, the spherical bubble solutions turn out to be unstable *versus* fission. This has been shown in nuclear physics quite some time ago [22]. In a recent work [23], we found that spherical nuclear bubbles may be stabilized by shell effects. In this paper, we show that the same is true for charged metal clusters if the number of valence electrons corresponds to a closed shell.

Recently, the experimental group at the MPI of Stuttgart [24] succeeded in producing fullerenes C_{60} covered by a layer of N Cs-atoms with $N \leq 500$. They also calculated [25] the electronic shell structure using a local approximation to the density-functional theory and discussed the measured abundances of metal-coated

* This work is partly supported by the Polish Committee of Scientific Research under contract No. 2P3 03B 49 09.

[a] e-mail: pomorski@nuclid.umcs.lublin.pl

fullerenes $C_{60}Cs(N)$ in terms of the magic numbers corresponding to the electronic shell closures in the metal layer. In the case of metal-coated fullerenes, the fullerene stabilizes the metal layer against deformation. One could imagine that, in the near future, metal layers could be produced on top of compact spherical (or deformed) mesoscopic aggregates of some insulating material. In this way, the electronic shell effects in the metal layer could be studied as a function of the geometry of the supporting material and of the number of metal atoms.

In our paper, we want to show that for large enough net charge and for magic numbers of free electrons, metallic bubbles may exist and may be stable against fission without the presence of a stabilizing fullerene skeleton.

In Section 2, we define the theoretical model and in Section 3 we present the results we obtained. Section 4 contains a short summary and a discussion of open questions.

2 Theoretical model

For mesoscopic metallic clusters containing from 100 to more than 1000 atoms, the distribution of the positively charged ions can be approximately described by a homogeneously smeared-out density which in the simplest case is given by a step function. For a bubble with inner radius R_2 and outer radius R_1, the density of positive ions is thus given by

$$\rho_{ion}(r) = \overset{\circ}{\rho}_{ion}\, \theta_0(r-R_2)\, \theta_0(R_1-r), \tag{2.1}$$

$$\theta_0(x) = \begin{cases} 1 \text{ for } x > 0 \\ 0 \text{ for } x < 0 \end{cases}.$$

The constant bulk density $\overset{\circ}{\rho}_{ion} > 0$ is usually given in terms of the radius $\overset{\circ}{r}_s$ of a sphere which contains 1 atom on the average

$$\overset{\circ}{r}_s = \left[\frac{3}{4\pi\, \overset{\circ}{\rho}_{ion}}\right]^{1/3}. \tag{2.2}$$

For a given number n of atoms, the volume of the bubble layer has to be equal to the one of a compact spherical cluster of radius R_0

$$\frac{4\pi}{3}(R_1^3 - R_2^3)\, \overset{\circ}{\rho}_{ion} = \frac{4\pi}{3} R_0^3\, \overset{\circ}{\rho}_{ion} = n. \tag{2.3}$$

Consequently, the shape of the spherical bubble is determined by only one free parameter. We choose it to be the ratio

$$f := R_2^3/R_1^3 \tag{2.4}$$

between the volume of the inner hole to the volume of the entire bubble or to be the dimensionless inner radius v_2

$$v_2 := \frac{R_2}{R_0} \tag{2.4'}$$

of the bubble.

The conduction electrons move independently in an average potential $V(r)$ which represents the mean interaction of a given electron with all the other electrons and with the positive background charge $\rho_{ion}(r)$. In the Hartree-Fock approximation the single particle states $\varphi_\nu(\mathbf{r})$ of the electrons[1] and the corresponding single particle energies ε_ν are obtained as the selfconsistent solution of the coupled equations

$$\left[-\frac{\hbar^2}{2m}\triangle + \widehat{V}(r)\right]\varphi_\nu(\mathbf{r}) = \varepsilon_\nu \varphi_\nu(\mathbf{r}), \tag{2.5}$$

$$\widehat{V}(r)\varphi_\nu(\mathbf{r}) = \left[V_{ion}(r) + \widehat{V}_e(r)\right]\varphi_\nu(\mathbf{r}), \tag{2.6}$$

$$V_{ion}(r) = -\int dr'\, \frac{\rho_{ion}(r')}{|\mathbf{r}-\mathbf{r}'|}, \tag{2.7}$$

$$\widehat{V}_e(r)\varphi_\nu(\mathbf{r}) = \sum_{\kappa\neq\nu} n_\kappa \int d^3r' \varphi_\kappa^\dagger(\mathbf{r}') \frac{e_0^2}{|\mathbf{r}-\mathbf{r}'|} \times \left[\varphi_\kappa(\mathbf{r}')\varphi_\nu(\mathbf{r}) - \varphi_\nu(\mathbf{r}')\varphi_\kappa(\mathbf{r})\right]. \tag{2.8}$$

In (2.8), e_0 is the elementary charge and n_κ is the occupation number of the single particle state φ_κ. For temperature $T = 0$, n_κ is given by

$$\begin{aligned} n_\kappa &= 1 \quad \text{for} \quad \varepsilon_\kappa \leq \varepsilon_F; \\ n_\kappa &= 0 \quad \text{for} \quad \varepsilon_\kappa > \varepsilon_F, \end{aligned} \tag{2.9}$$

where ε_F is the Fermi energy. We assume that the temperature is zero.

The Hartree-Fock potential (2.8) is seen to be state-dependent mainly due to the exchange term. Usually, the exchange term is replaced by a local density approximation [3,26]. If we neglect the exchange term altogether and suppress the exclusion of the state $\varphi_\kappa = \varphi_\nu$ in the remaining Hartree potential, we obtain

$$\widehat{V}_e(r)\varphi_\nu(\mathbf{r}) = \int d^3r' \frac{\rho_e^H(r')e_0}{|\mathbf{r}-\mathbf{r}'|}\varphi_\nu(\mathbf{r}), \tag{2.10}$$

$$\rho_e^H(r') = \sum_\kappa n_\kappa\, e_0 \varphi_\kappa^\dagger(\mathbf{r}')\, \varphi_\kappa(\mathbf{r}'). \tag{2.11}$$

The solution of the remaining set of selfconsistent Hartree equations (Eqs. (2.5) with (2.6, 2.7, 2.10, 2.11)) is still a considerable technical problem. It has been carried through for instance in reference [3].

A great simplification is obtained if the selfconsistent average potential (2.6) is replaced by a phenomenological ansatz. Most of the shell structure calculations for compact metal clusters have been performed on the basis of simple phenomenological potentials, in particular the Nilsson potential [6,9], the Saxon-Woods potential [7,11], and the "wine-bottle" potential [7]. It can indeed be seen from the results of reference [3] that for atom numbers $n \geq 40$ the selfonsistently calculated potential $V(r)$ resembles a Saxon-Woods potential and roughly even to

[1] We leave away an explicit notation of the spin degrees because spin-dependent interactions are neglected.

a square well. We, therefore, felt justified to represent the average potential $V(r)$ for the case of a bubble cluster by an infinite square well with the boundaries given by the distribution of the positive ions

$$V(r) = \begin{cases} -V_0 \ \text{for} R_2 < r < R_1 \\ +\infty \ \text{otherwise} \end{cases} . \tag{2.12}$$

This simple choice of the shell model potential has the great advantage that the eigenfunctions of the Schrödinger equation (2.5) are linear combinations of spherical Bessel- and Neumann functions and the eigenenergies ε_ν are easily obtained from the boundary conditions at $r = R_{1,2}$ [23]. Furthermore, the single particle energies of the infinite square well exhibit a scaling property: they depend on the number on the number n of atoms as $\varepsilon_\nu = \varepsilon_\nu \left[n^{-2/3}\right]$. Consequently, using the energy unit $\left[n^{-2/3}\right]$ eV, the level scheme is valid for all sizes of the system (see Fig. 3).

The well depth V_0 in (2.12) is of the order of 0.5 Ry (1 Ry = 13.6 eV). Its value is not relevant for our results because the shell correction energy (see Eq. (2.16)) turns out to be independent of the constant V_0.

We now have to determine the total energy E_{tot} of the metal cluster as a function of the variable f (see Eq. (2.4)). Given the fact that the ion density $\rho_{ion}(r)$ can be considered to be constant inside the matter distribution (see (2.1)), we may write the energy of the system as a sum of the energy E_{LD} of a "liquid drop" and a "shell correction energy" E_{shell} following Strutinsky [13]

$$E_{tot} = E_{LD} + E_{shell}. \tag{2.13}$$

The liquid drop energy can be written as a sum of a (negative) term proportional to the volume V of the system and a (positive) term proportional to the surface S. We note that the coefficients τ and σ in the expression for the LD-energy contain the effects of the ions *and* of the free electrons. The electronic contribution to these parameters can be obtained in the Thomas-Fermi (TF) approximation. We use empirical values for τ and σ as obtained for macroscopic systems. They thus represent the sum of the ionic and electronic contributions.

Since we consider (positively) charged clusters, we have to add the electrostatic energy E_{Cb} of the system

$$E_{LD} = -\tau V + \sigma S + E_{Cb} \tag{2.14}$$

which turns out to be a much bigger term than in a neutral cluster.

Some authors [10] include a term proportional to the average curvature of the surface which is the 3rd term in the expansion of the energy-density functional of a leptodermous system in terms of $n^{-1/3}$. In the case of a bubble shape, the curvature terms arising from the inner and outer surface have opposite signs beside the fact that their absolute value is much smaller than the corresponding surface term. We omit the curvature term thereby following reference [21]. Consideration of the curvature term would favour spherical bubbles as compared to compact spheres.

The "macroscopic" electrostatic energy E_{Cb} is given as a function of smooth density distributions of the positive and negative charge by

$$E_{Cb} = \frac{1}{2} \int d^3r \int d^3r' \frac{[\rho_e(r) - \rho_{ion}(r)][\rho_e(r') - \rho_{ion}(r')]}{|\mathbf{r} - \mathbf{r}'|} \tag{2.15}$$

and the shell-correction energy E_{shell} as a function of the single-particle energies ε_κ by

$$E_{shell} = \sum_\kappa \varepsilon_\kappa (n_\kappa - \bar{n}_\kappa), \tag{2.16}$$

where the occupation probabilities n_κ were defined in (2.9), whereas the quantities $\bar{n}_\kappa$ represent smooth occupation probabilities in a cluster in which the shell structure is washed out using the Strutinsky prescription [13].

In our simple phenomenological model, we represent the distribution of the positive surplus charge $[\rho_{ion}(r) - \rho_e(r)]$ by a simple ansatz: from classical electrodynamics we know that the surplus charge ought to be localized at the outer surface of the metallic bubble. We, therefore, assume the total (positive) surplus charge qe_0 to be distributed in a thin layer of thickness ε along the outer surface

$$[\rho_{ion}(r) - \rho_e(r)] = \delta\rho\, \theta_0(r - (R_1 - \varepsilon))\, \theta_0(R_1 - r), \tag{2.17}$$

where

$$\delta\rho = \frac{3qe_0}{4\pi[R_1^3 - (R_1 - \varepsilon)^3]} .$$

Calculating the Coulomb energy (2.15) for this distribution as a function of the small quantity $\eta_1 = \varepsilon/R_1$, we obtain

$$E_{Cb} = \frac{(4\pi\delta\rho)^2 R_1^5}{3} \Big\{ \frac{1}{5}[1 - (1 - \eta_1)^5] - \frac{1}{2}(1 - \eta_1)^3 (2\eta_1 - \eta_1^2) \Big\},$$

or

$$E_{Cb} = \frac{q^2 e_0^2}{2R_1} \frac{\left[1 - \frac{5}{3}\eta_1 + \eta_1^2 - \frac{1}{3}\eta_1^3\right]}{\left[1 - 2\eta_1 + \frac{5}{3}\eta_1^2 - \frac{2}{3}\eta_1^3 + \frac{1}{9}\eta_1^4\right]} . \tag{2.18}$$

Up to terms of the order η_1^2 this can be written

$$E_{Cb} = \frac{q^2 e_0^2}{2R_1} \left[1 + \frac{\eta_1}{3} + \Theta(\eta_1^3)\right]. \tag{2.19}$$

The term of order $(\varepsilon/R_1)^0$ in (2.19) represents the Coulomb energy in the limit that the surplus charge is located in an infinitely thin layer at the outer surface. One sees from (2.19) that in 1st order the Coulomb energy increases if the surplus charge is distributed homogeneously in a layer of *finite* thickness $\varepsilon \ll R_1$. Consequently, we used the Coulomb energy in zeroth order of ε/R_1 in our calculations.

The total energy of the spherical metallic bubble has thus the form

$$E_{tot} = -\tau\frac{4\pi}{3}(R_1^3 - R_2^3) + \sigma 4\pi(R_1^2 + R_2^2) + \frac{q^2e_0^2}{2R_1} + E_{shell}(f). \tag{2.20}$$

Subtracting from this expression the energy of a compact spherical cluster of the same charge qe_0 and the same volume we obtain

$$\Delta E(f;q) := \Delta E_{LD}(f;q) + \Delta E_{shell}(f;n-q), \tag{2.21}$$

where

$$\Delta E_{LD}(f;q) = 4\pi\sigma\left(R_1^2 + R_2^2 - R_0^2\right) + \frac{q^2e_0^2}{2}\left(\frac{1}{R_1} - \frac{1}{R_0}\right) \tag{2.21'}$$

and

$$\Delta E_{shell}(f;n-q) = E_{shell}(f;n-q) - E_{shell}(0;n-q). \tag{2.21"}$$

We note that the single particle potential (2.12) becomes a simple central square-well in the limit $R_2 \to 0$ (*i.e.* $f \to 0$). Thus the shell correction energy $E_{shell}(f=0)$ is obtained by substituting the eigenvalues $\varepsilon_\kappa(f=0)$ in a simple central well with infinite wall at $r = R_0$. The occupation probabilities have to be chosen in each case according to Strutinsky's prescription.

The 1st term and 2nd term of (2.21') are simple functions of the parameter f due to the relations

$$R_1 = R_0\left(\frac{1}{1-f}\right)^{1/3}, \tag{2.22}$$

$$R_2 = R_0\left(\frac{f}{1-f}\right)^{1/3}. \tag{2.22'}$$

The radius R_0 of the compact spherical cluster is related to the number of n of atoms by

$$R_0 = \overset{\circ}{r}_s\ n^{1/3} \tag{2.23}$$

with the radius parameter given in (2.2).

The surface tension σ and the radius $\overset{\circ}{r}_s$ of the Wigner-Seitz cell are thus the only parameters which specify a given metal in our model.

The difference $\Delta E_{LD}(f;q)$ between the LD-energies of the compact cluster and the bubble (Eq. (2.21')) is seen to consist of a positive term describing the increase of the surface energy and a negative term which represents the reduction of the repulsive Coulomb energy. As far as the "macroscopic" part of the energy is concerned, a preference for the bubble geometry may only occur through the reduction of the Coulomb energy which increases with the surplus charge q of the metal cluster. For a given metal and a given "size" n of the cluster there will thus be a critical value q_c of the charge at which the (spherical) bubble becomes the configuration of lower energy. It will depend on the type of the metal (*i.e.* on the value of the surface tension σ and the radius parameter $\overset{\circ}{r}_s$) whether the cluster is still stable *versus* fission or emission of atoms at this value of the charge.

The difference ΔE_{shell} of the shell correction terms can be positive or negative. If the number $(n-q)$ of valence electrons happens to be a magic number for the bubble geometry, and not for the compact spherical form, ΔE_{shell} will be a negative number and thus favour the formation of a bubble a.v.v.

The question whether, for given charge, the bubble has a lower energy than the compact sphere, depends sensitively on the value of the surface constant σ and the radius parameter $\overset{\circ}{r}_s$. More precisely, it depends on the "fissility" parameter which is defined to be the ratio of the Coulomb energy E_{Cb} and twice the surface energy E_S. The factor 2 is inserted in order to retain the definition used in nuclear physics:

$$X = \frac{E_{Cb}(f)}{2E_S(f)} = \frac{q^2e_0^2}{16\pi\sigma R_1(R_1^2 + R_2^2)} = X_0\left(\frac{1-f}{1+f^{2/3}}\right), \tag{2.24}$$

with X_0, the fissility parameter of a compact sphere, being defined by

$$X_0 = \frac{E_{Cb}(f=0)}{2E_S(f=0)} = \frac{q^2e_0^2}{16\pi\sigma\ \overset{\circ}{r}_s^{\,3}\ n}\cdot \tag{2.25}$$

The difference ΔE_{LD} between the energy of the spherical bubble and of the compact spherical cluster (see (2.21')) measured in units of $2E_S(f=0)$ is given as a function of the ratio $f = (R_2/R_1)^3$ or of the dimensionless inner radius $v_2 = R_2/R_0$ by the functions

$$\begin{aligned} F :&= \frac{\Delta E_{LD}(f;q)}{2E_S(f=0)} \\ &= \frac{1}{2(1-f)^{2/3}}\left[1 + f^{2/3} - (1-f)^{2/3}\right] \\ &\quad - X_0\left[1 - (1-f)^{1/3}\right] \end{aligned} \tag{2.26}$$

and

$$\begin{aligned} F &= \frac{\Delta E_{LD}(v_2;q)}{2E_S(v_2=0)} \\ &= \frac{1}{2}\Big[(1+v_2^3)^{2/3} + v_2^2 - 1\Big] - X_0\Big[1 - (1+v_2^3)^{-1/3}\Big], \end{aligned} \tag{2.26'}$$

resp. The 1st terms on the r.h.s. of the equations (2.26, 2.26') are positive and the 2nd terms are negative. Clearly, for large enough X_0, the function F becomes negative, *i.e.* the bubble shape corresponds to a lower energy. The stationarity conditions

$$\frac{\partial F}{\partial f} = 0 \tag{2.27}$$

and

$$\frac{\partial F}{\partial v_2} = 0 \tag{2.27'}$$

resp., in any case exhibit the "trivial" solution $f = v_2 = 0$. This means that the compact spherical aggregate always corresponds to a stationary value of the energy. Additional "non-trivial" physical solutions exist if the stationarity condition

$$1 + f^{1/3} - X_0 f^{1/3}(1-f) = 0 \tag{2.28}$$

or

$$1 + \frac{v_2}{(1+v_2^3)^{1/3}} - X_0 \frac{v_2}{(1+v_2^3)^{4/3}} = 0 \tag{2.28'}$$

has real roots in the range $0 < f < 1$ or $v_2 > 0$, resp. It is easily seen that such solutions exist only if the fissility parameter $X_0 > 3.379$. We note that in the case of nuclei, which exhibit a *homogeneous* charge distribution, the corresponding non-trivial solutions occur for $X_0 > 2.2$ (see Ref. [23]). The function $F(v_2)$ and the solution $X_0(v_2)$ of equation (2.28') will be shown and discussed in Section 3.

Let us now turn to the important question of how the total energy depends on the deformation: it can be easily shown that the LD-energy of a bubble decreases as a function of deformation because the decrease of the repulsive electrostatic energy turns out to be greater than the increase of the surface energy. A spherical bubble may, however, be stabilized against deformation by shell effects. If the $(n-q)$ valence electrons of the charged metal bubble correspond to a closed shell configuration in the spherically symmetric potential (2.12), the shell energy yields an additional binding of a couple of eV. As one deforms the bubble the absolute value of this negative shell energy decreases as a function of deformation. In this way a barrier against fission is produced. The calculation of the total energy of the bubble as a function of the deformation implies that we determine the eigenvalues in a deformed bubble potential. This is a difficult task if we were to tackle it in full generality. There is, however, a family of deformed shapes which can be transformed into a spherical shape by a scaling transformation. For this "scaling model", it is relatively simple to calculate the eigenvalues:

Assume that the outer (S_1) and inner (S_2) surface of the deformed bubble are concentric spheroids with the half-axes $a_{1(2)}$ and $c_{1(2)}$

$$S_{1(2)}: \frac{x^2+y^2}{a_{1(2)}^2} + \frac{z^2}{c_{1(2)}^2} = 1 \tag{2.29}$$

enclosing the constant volume $\frac{4\pi}{3}(R_1^3 - R_2^3)$

$$R_0^3 = R_1^3 - R_2^3 = a_1^2\, c_1 - a_2^2 c_2. \tag{2.30}$$

An infinite square well with the boundaries (2.29)

$$\hat{V}(x,y,z) = -V_0\, \eta_0(\mathbf{x}), \tag{2.31}$$

where

$$\eta_0(\mathbf{x}) = \begin{cases} 1 & \text{for } \mathbf{x} \in \text{volume } \Omega \text{ enclosed by } S_1 \text{ and } S_2 \\ -\infty & \text{otherwise} \end{cases}$$

transforms into a simple spherically symmetric potential of the type (2.12) which depends on the scaled variable

$$\xi = \lambda x; \quad \eta = \lambda y; \quad \zeta = \mu z \tag{2.32}$$

or the corresponding polar variables ρ, ϑ, φ

$$\xi = \rho\, \sin\vartheta\, \cos\varphi; \quad \eta = \rho\, \sin\vartheta\, \sin\varphi; \quad \xi = \rho \cos\vartheta. \tag{2.32'}$$

The 2 scaling parameters λ, μ are related to each other by the constraint (2.30) which takes the form

$$\lambda^2 \mu = 1. \tag{2.33}$$

Thus they can be expressed by a single deformation parameter. Using the deformation parameter δ introduced by Nilsson in reference [27] the scaling parameters are given as a function of δ by

$$\lambda = \left(\frac{1+\frac{2}{3}\delta}{1-\frac{4}{3}\delta}\right)^{\frac{1}{6}} \qquad \mu = \left(\frac{1-\frac{4}{3}\delta}{1+\frac{2}{3}\delta}\right)^{\frac{1}{3}}. \tag{2.34}$$

In the scaled variables, the Schrödinger equation takes the form

$$(\hat{H}_0 + \hat{H}_1)\varphi_\nu = \varepsilon_\nu\, \varphi_\nu. \tag{2.35}$$

The Hamiltonian $\hat{H}_0$ is spherically symmetric in the ξ, η, ζ coordinates

$$\hat{H}_0 = -\frac{\hbar^2}{2M_\delta}\, \Delta_{\xi\eta\zeta} + V(\rho), \tag{2.36}$$

where $\Delta_{\xi\eta\zeta}$ is the Laplacian operator in ξ, η, ζ space and

$$M_\delta = M\Big(1+\frac{2}{3}\delta\Big)^{\frac{2}{3}}\Big(1-\frac{4}{3}\delta\Big)^{\frac{1}{3}}. \tag{2.37}$$

The scaled square well potential is now spherical

$$V(\rho) = \begin{cases} -V_0 \text{ for } & R_2 < \rho < R_1 \\ +\infty \text{ otherwise} & \end{cases}. \tag{2.38}$$

The term $\hat{H}_1$ in (2.35) represents the deformation dependent part of the Hamiltonian

$$\hat{H}_1 = \frac{2}{3}\delta \frac{\hbar^2}{2M_\delta}\left(2\frac{\partial^2}{\partial\zeta^2} - \frac{\partial^2}{\partial\xi^2} - \frac{\partial^2}{\partial\eta^2}\right). \tag{2.39}$$

For determining the stability of a spherical bubble with respect to elongation, we only need to consider small deformations δ. Consequently, we may treat $\hat{H}_1$ as a perturbation. This means that the single-particle energy ε_ν can

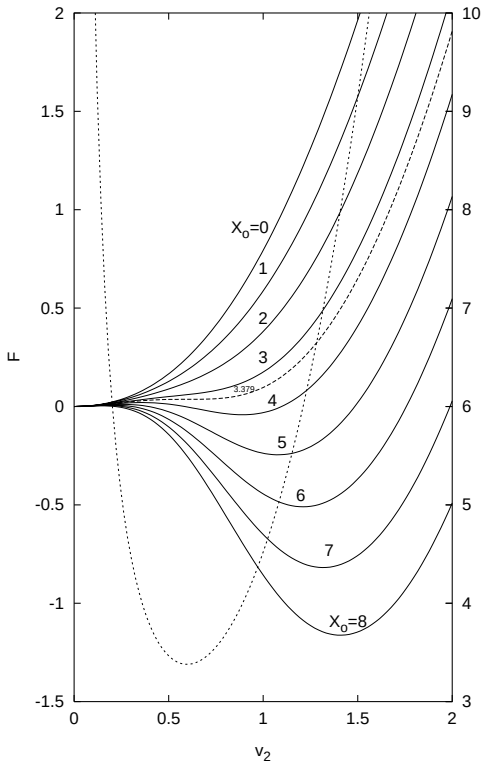

Fig. 1. Dimensionless energy difference F (see Eq. (2.26')) as a function of the dimensionless inner radius $v_2 = R_2/R_0$ of the bubble for different values of the fissility parameter X_0 (see Eq. (2.25)). We also show the solution $X_0(v_2)$ of the stationarity condition (2.28') by the dashed curve with X_0 plotted on the vertical axis (see scale on the right-hand side of the figure).

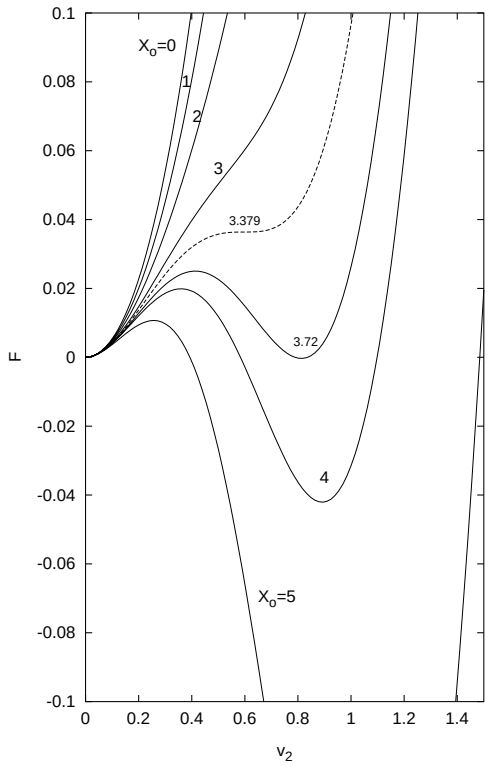

Fig. 2. Same plot as Figure 1 but with larger scale on the vertical axis. Notice that for fissility parameters $3.379 \leq X_0 \leq 3.72$ the bubble solution corresponds to a higher energy than the compact sphere and for $X_0 \geq 3.72$ to a lower one.

be approximately obtained as a function of the eigenenergies $\overset{\circ}{\varepsilon}_\nu$ and eigenfunctions $\overset{\circ}{\varphi}_\nu$ of the Hamiltonian $\hat{H}_0$:

$$\varepsilon_\nu \approx \overset{\circ}{\varepsilon}_\nu + \langle \overset{\circ}{\varphi}_\nu | \hat{H}_1 | \overset{\circ}{\varphi}_\nu \rangle. \tag{2.40}$$

For larger deformations, one has to diagonalize $\hat{H}_1$ in the basis of the s.p. states $\overset{\circ}{\varphi}_\nu$. In all the results shown in Section 3, the eigenvalues ε_ν were determined by diagonalization of $\hat{H}_1$ in a sufficiently large subspace of s.p. states $\overset{\circ}{\varphi}_\nu$.

The matrix-elements of $\hat{H}_1$ can be easily evaluated if we make use of the following operator equation which can be derived in a straightforward way:

$$\begin{aligned} 2\frac{\partial^2}{\partial\zeta^2} - \frac{\partial^2}{\xi^2} - \frac{\partial^2}{\eta^2} &= \frac{1}{8}\left[\Delta_{\xi\eta\zeta}, \left[\Delta_{\xi\eta\zeta}, 2\rho^2 P_2(\cos\vartheta)\right]\right] \\ &= \frac{1}{8}\left(\frac{2M_\delta}{\hbar}\right)^2 [\hat{H}_0, [\hat{H}_0, 2\rho^2 P_2(\cos\vartheta)]] \\ &\quad + \frac{M_\delta}{\hbar^2}(3\zeta^2 - \rho^2)\frac{1}{\rho}\frac{\partial V}{\partial \rho}\,. \end{aligned} \tag{2.41}$$

The relation (2.41) holds for any choice of a spherically symmetric potential $V(\rho)$. In the case of the infinite square well (2.38), the derivative $\dfrac{\partial V}{\partial \rho}$ is given by

$$\frac{\partial V}{\partial \rho} = V_0[\delta(\rho - R_1) - \delta(\rho - R_2)]. \tag{2.41'}$$

As the eigenfunctions $\overset{\circ}{\varphi}_v$ of $\hat{H}_0$ vanish at $\rho = R_{1,2}$, the 2nd term on the r.h.s. of (2.41) does not contribute. Simple algebra leads to the expression

$$\langle \overset{\circ}{\varphi}_\nu | \hat{H}_1 | \overset{\circ}{\varphi}_\mu \rangle = \frac{\delta}{6}\left(\frac{2M_\delta}{\hbar^2}\right)(\overset{\circ}{e}_\nu - \overset{\circ}{e}_\mu)^2 \langle \overset{\circ}{\varphi}_\nu | \rho^2 P_2(cos\theta) | \overset{\circ}{\varphi}_\mu \rangle. \tag{2.42}$$

The matrix elements of ρ^2 where evaluated numerically, while the matrix elements of spherical harmonics are expressed in terms of Clebsch-Gordan coefficients.

3 Results

It is useful to consider first the results obtained within the pure liquid drop (LD) model separately because they present the average trends as a function of the net charge number q and the number n of atoms.

In Figures 1 and 2 we show the dimensionless energy F as a function of the dimensionless inner radius $v_2 = R_2/R_0$

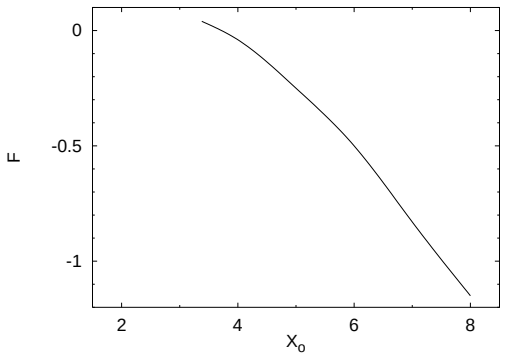

Fig. 3. Energy difference F between the bubble solution and the compact sphere as a function of the fissility parameter X_0 (Eq. (2.25)).

for different values of the fissility parameter X_0. Furthermore, in Figure 1, we exhibit the solution $X_0(v_2)$ or equation (2.28') which for any given value $X_0 > 3.379$ yields two real values of v_2, where F is stationary. The larger one corresponds to the bubble solution and the smaller one to the potential barrier which is located between the solutions pertaining to the compact sphere ($v_2 = 0$) and to the bubble. In particular, inspection of the solution $X_0(v_2)$ of equation (2.28') tells us that whenever a bubble solution exists, there is always a barrier which separates it from the compact sphere solution. The maximal barrier height is given by $F = 0.037$. In a tiny range of fissility parameters ($3.379 < X_0 \leq 3.72$), the energy of the bubble solution turns out to be higher than the energy of the compact sphere. With increasing X_0 the energy of the bubble solution decreases. In Figure 3, we show the energy difference F of the bubble solution compared to the compact sphere as a function of the fissility parameter X_0.

In order to obtain the energy F in ordinary units one has to multiply F with 2 times the surface energy E_S of the compact sphere:

$$2E_S = 8\pi\sigma \overset{\circ}{r}{}_s^2 \, n^{2/3} = \begin{cases} 3,25 \text{ eV} \times n^{2/3} \text{ for } {}^{23}\text{Na} \\ 1,23 \text{ eV} \times n^{2/3} \text{ for } {}^{133}\text{Cs}. \end{cases}$$

At fissility $X_0 = 4$ and for cluster sizes of $n = 100$ and $n = 1000$ we obtain the following gains in binding energy due to forming a bubble instead of a compact sphere: $|F|2E_S = 2.8$ eV and 13 eV, resp., for ^{23}Na

$|F|2E_s = 1.05$ eV and 4.92 eV, resp., for ^{133}Cs. Unfortunately, the charges necessary for obtaining bubble solutions are quite high. This can be checked by noticing that X_0 can be written in the form

$$X_0 = \frac{(q^2/n)}{(q^2/n)_c}, \tag{3.1}$$

where

$$(q^2/n)_c := \frac{16\pi\sigma \overset{\circ}{r}{}_s^3}{e_0^2} = \begin{cases} 0.934 \text{ for Na} \\ 0.509 \text{ for Cs.} \end{cases} \tag{3.2}$$

For a system with fissility parameter $X_0 = 4$, this implies the following values of q^2/n for the two metals Na and Cs:

$$\left(\frac{q^2}{n}\right)_{X_0=4} = \begin{cases} 3.74 \text{ for Na} \\ 2.04 \text{ for Cs.} \end{cases} \tag{3.3}$$

We must keep in mind that these results obtained within a simple LD model only indicate the *average trends*. Substantial changes are produced by the shell structure whenever the number $(n - q)$ of free electrons corresponds to a shell closure for the bubble-shaped nucleus. In this case, the shell effect may favour the spherical bubble *versus* the compact sphere already at smaller net charges of the cluster. In addition, the shell effect is of crucial importance for stabilizing the spherical charged metal bubbles against fission. This will be investigated later.

We performed calculations for metallic agglomerates of sodium (^{23}Na) and of Cesium (^{133}Cs). The following empirical values of the LD-parameters [21,28] were used:

$$\begin{aligned} {}^{23}\text{Na}\colon \overset{\circ}{r}_s &= 2.07 \text{ Å}; \qquad \tau = 0.03017 \text{ eV Å}^{-3}; \\ \sigma &= 0.01894 \text{ eV Å}^{-2} \\ {}^{133}Cs\colon \overset{\circ}{r}_s &= 2.98 \text{ Å}; \qquad \tau = 0.00722 \text{ eV Å}^{-3}; \\ \sigma &= 0.00550 \text{ eV Å}^{-2} \end{aligned}$$

The LDM results for the binding energy (E_{LD}, Eq. (2.14)), the energy gain (ΔE_{LD}, Eq. (2.21')) by bubble formation, the fissility parameter X (Eq. (2.24)) and the hole fraction (Eq. (2.4)) for the bubble solution are shown as a function of the number n of atoms in the cluster in Figure 4 for Na and in Figure 5 for Cs. Different curves correspond to different numbers q of the net (positive) charge of the cluster. It is seen that only for quite massive and highly charged clusters the bubble configuration has a lower energy than the compact sphere. The hole fraction f varies from 0.3 to 0.9, the hole being the larger, the greater the net charge q for given number n of atoms.

In all cases of LD-bubble solutions, the fissility parameter X of the bubble (Eq. (2.24)) turns out to be larger than 1. This implies that within the LD model there is no fission barrier on the way from the spherical bubble to fission. Only the shell energy may lead to a stabilization of the spherical bubble solution against fission in very much the same way as this has been shown to be the case for nuclear bubbles [23]. The scheme of electronic levels which is obtained for the infinite square well potential (2.12), is shown in Figure 6 as a function of the hole fraction f (Eq. (2.4)). The infinite square well has the advantage that its eigenvalues scale with $n^{-2/3}$. Therefore, with the energy unit used in Figure 6, the level scheme is universally valid for all cluster sizes n except for the $1/\overset{\circ}{r}{}_s^2$ dependence of the levels on the value of the Wigner-Seitz parameter $\overset{\circ}{r}_s$. In the plot of Figure 6, we chose the radius parameter of Cs.

We draw the attention of the reader to the fact that the levels with node number $n > 1$ rise much more steeply as a function of increasing hole parameter f than the levels

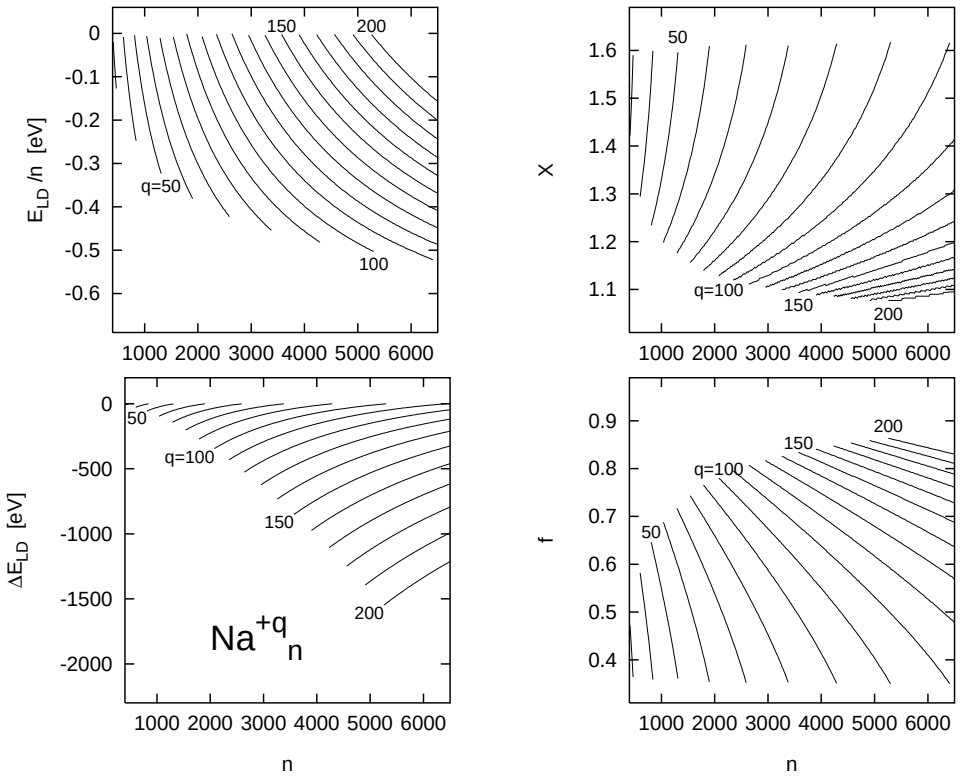

Fig. 4. Liquid drop results for the binding energy (E_{LD}, Eq. (2.1)), energy gain (ΔE_{LD}, Eq. (2.21')) with respect to the energy of a compact spherical cluster, fissility parameter (X, Eq. (2.24)) and the equilibrium hole fraction (f, Eq. (2.4)) for the charged ($q\, e_0$) sodium cluster with the bubble structure as function of n.

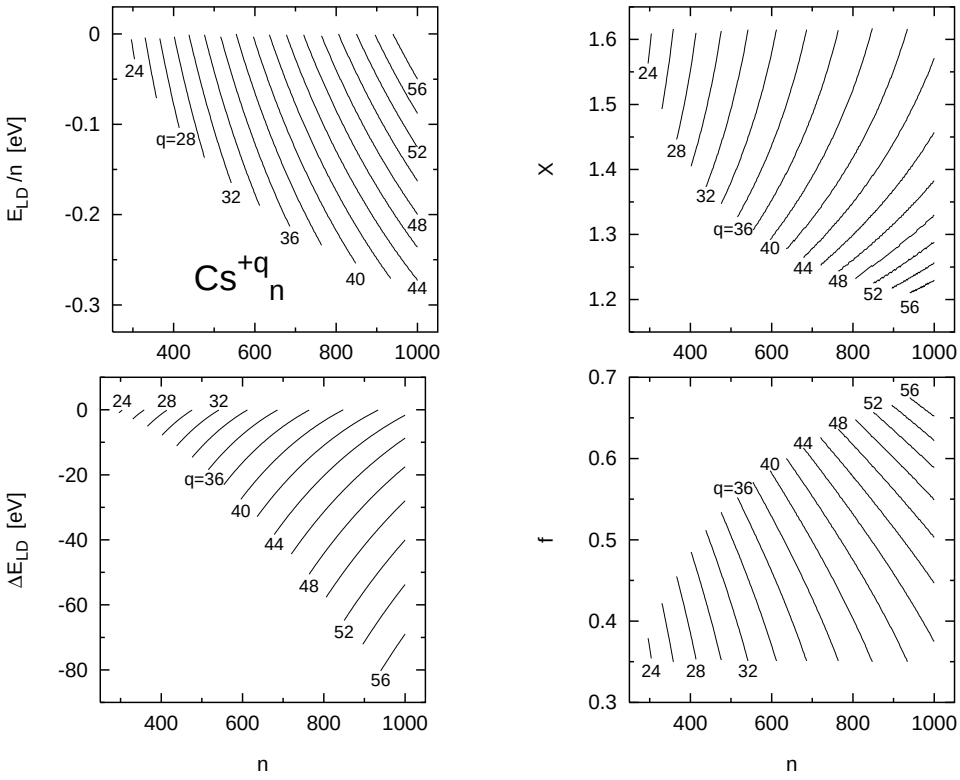

Fig. 5. The same as in Figure 4 but for charged clusters of cesium.

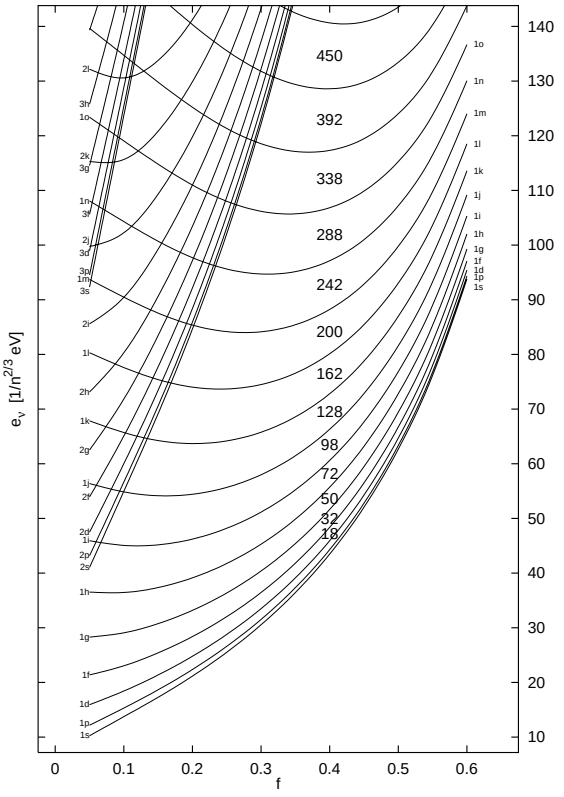

Fig. 6. Electronic level scheme as a function of the hole fraction $f = (R_2/R_1)^3$ for the infinite spherical square well (2.12). The energy unit used takes into account that the eigenvalues of the infinite square well scale with $n^{-2/3}$. The radius constant $\mathring{r}_s$= 2.98 Å is used in the plot.

with node number $n = 1$. The physical reason of this phenomenon is that for s.p. states which exhibit one or several radial nodes within the metallic layer, the kinetic energy increases much more with decreasing thickness of the layer than for s.p. states without such a radial node. This is a general feature of the level scheme of a bubble-shaped potential. It occurs in a similar way if we use a harmonic oscillator instead of a square well [23].

Within the group of levels with given node number n, the only other quantum number entering the single particle energies is the orbital angular momentum l with a degeneracy factor of $2(2l + 1)$. The gaps between shells of neighbouring l values become larger with increasing l value. For a purely metallic bubble and the choice of the simple square well potential, the magic numbers are given by

$$\sum_{l=0}^{l_0} 2(2l + 1) = 2(l_0 + 1)^2,$$

where l_0 is the largest orbital angular momentum still occupied. For compact spherical cluster the number of radial nodes does not play any special role. Therefore, for compact spheres the shell closures are determined by the principal quantum number.

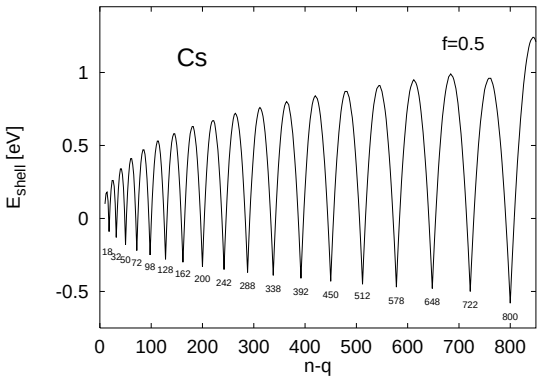

Fig. 7. Shell correction energy for the Cs bubble cluster with the hole fraction $f = 0.5$ as a function of $n - q$.

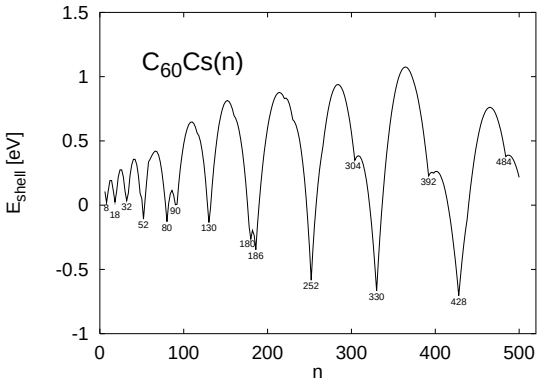

Fig. 8. Shell energy for a (neutral) Cs-coated fullerene $C_{60}Cs(n)$ as a function of the number n of free electrons residing in the metallic layer.

We note that the orbital angular momenta l_0 for the topmost electrons are large. So, for a bubble-shaped cluster of 242 free electrons, the topmost angular momentum is $l_0 = 10$ with a degeneracy of 42.

In principle there will also be shell closures for states with higher radial node number. However, they occur at smaller values of the hole parameter f (see Fig. 6), where the LD energy does not yet contribute enough energy gain. If we were to plot the LD-energy difference F of Figures 1 and 2 as a function of f rather than v_2, the bubble valleys would occur for f-values in the range $0.4 \leq f \leq 0.7$. The shell energy (2.16) is plotted as a function of the number $n - q$ of free electrons in Figure 7. The plot is for Cs and for the value $f = 0.5$ of the hole parameter. For Na and other metals the corresponding plot looks very similar. The minima of the shell energy for spherical bubbles occur at the magic numbers

$$\mathcal{M}_{bubble} = 2,\ 8,\ 18,\ 32,\ 50,\ 72,\ 98,\ 128,\ 162,\ 200,\ 242,\ 288,\ 338,\ 392,\ 450,\ 512,\ 578,\ 648,\ 722, \ldots$$

which differ from the magic numbers obtained for compact spherical cluster [29]

$$\mathcal{M}_{comp} = 2,\ 8,\ 20,\ 34,\ 50,\ 92,\ 138,\ 190,\ 254,\ 338,\ 438,\ 546,\ 676,\ 832.$$

The shell energies for the magic numbers 450, 512, ..., 800 are seen to be of the order of -0.5 eV in Figure 7. For Na, the picture would look very similarly. We chose Na as one example clusters because a lot of experimental work exist on sodium cluster (see for instance Refs. [17–19]). The choice of Cs as 2nd example was motivated by the fact that recent experiments on Cs-coated fullerenes [24,25] demonstrated the existence of shell effects due to the conduction electrons in the metal layer for large enough numbers of Cs-atoms. The shell correction energy corresponding to the conduction electrons of the metallic layer on top of the C_{60}-fullerene were calculated recently by Springborg *et al.* [25]. This calculation is close to our work. In the case of the metal-coated fullerene, the metallic bubble is stabilized by the fullerene. Consequently, metal-coated fullerenes are expected to exist for a wide range of numbers n of metal atoms and a variety of metals. Shell effects can thus be studied by looking at the abundance distribution, as usual. The authors of reference [25] used a more sophisticated shell model potential than we do, which is obtained from a density functional approach.

In Figure 8 we present the results of our calculation of the shell energy in an uncharged layer of Cs-atoms on top of a C_{60}-fullerene. It is shown as a function of the number n of Cs atoms in the layer. The minima of the shell energy are seen to occur at values of n which differ from the magic numbers which we obtained for the purely metallic bubbles. This is due to the fact that for the metal-coated fullerene the inner radius R_2 is fixed by the fullerene ($R_2 = 3.57$ Å), whereas the outer radius R_1 changes as a function of the number of Cs atoms. Consequently, the hole parameter f is a function of n in Figure 8, whereas it is kept constant in Figure 7.

If one compares the magic numbers obtained in Figure 8 with the dips in the experimental photo-ionization spectra of $C_{60}Cs(n)$ clusters [25] one should keep in mind that the metallic Cs layer is expected to donate a limited number of free electrons to the fullerene. The authors of reference [25] assumed this number to be 6. If we adopt this hypothesis, then the number of Cs-ions in the metal layer for given magic numbers $n(\mathrm{mag})$ of free electrons in the layer is $(n(\mathrm{mag})+6)$. These ion numbers must be compared with the experimental ion numbers $N(\mathrm{dip})$ given in reference [25], where dips in the photo-ionization mass spectra of $C_{60}Cs(N)$ were observed.

The experimental numbers $N(\mathrm{dip})$ are [25]

$$N(\mathrm{dip}) = 12 \pm 0,\ 27 \pm 1,\ 33 \pm 1,\ 44 \pm 1,\ 61 \pm 1,\ 98 \pm 1,\ 146 \pm 2,\ 198 \pm 0,\ 255 \pm 5,\ 352 \pm 10,\ 445 \pm 10,$$

whereas our results corrected for the 6 donated electrons are (see Fig. 8)

$$n(\mathrm{mag}) + 6 = 14,\ 24,\ 38,\ 58,\ 86,\ 96,\ 136,\ 186,\ 192,\ 258,\ 336,\ 434.$$

The agreement is not good, but at higher mass numbers, where the jellium model is more reliable, there is undeniably a clear correspondence between the experimental and theoretical values. The calculated magic numbers in the more sophisticated model of reference [25] are closer to experiment than ours, but there are also discrepancies.

The main purpose our work is, however, not to contribute to the understanding of shell effects in metal-coated fullerenes but to establish the claim that purely metallic aggregates carrying a sufficiently high charge are more strongly bound in the form of bubbles rather than of compact spheres and are protected against fission by a fission barrier which owes its existence to the shell effect for the spherical bubble.

This claim is corroborated by the results of Figure 9 for a cluster of 482 Cs ions, carrying altogether 32 positive charges. The shell effect for the deformed bubble was calculated on the basis of the scaling model presented in Section 2. In Figure 9a we show the LD-energy for spherical bubbles as a function of the hole parameter f. The minimum is seen to correspond to the value $f = 0.45$. The spherical bubble corresponding to $f = 0.45$ is then deformed into axially symmetric spheroids described by the deformation parameter δ introduced by equation (2.34). The LD-energy E_{LD} is seen to decrease as a function of δ (see Fig. 9b), whereas the shell energy E_{shell}, which is negative (~ -0.6 eV) at sphericity, rises as a function of δ and passes a slightly positive maximum at $\delta \approx 0.2$ (see Fig. 9c). The total energy E_{tot} as a function of δ is shown in Figure 9d. It exhibits a barrier of about 0.7 eV height at a spheroidal deformation of $\delta \approx 0.2$. This is a small barrier height, which limits the tolerable temperatures to a couple of thousand °K. The decay by tunneling can be discarded because the inertia of the cluster is very large. The results for Na look similar. There are probably other metals which are more adapted to the formation of bubbles than the two cases we studied.

Which criteria of selecting a metal should be looked for?

Since the bubble formation requires a fissility parameter $X_0 > 3.3279$, at least as far as the LD model is concerned, one should look for systems with a small parameter $(q^2/n)_c$ (see Eq. (3.2)), which implies systems with a small surface tension σ and a small specific the volume $v_0 = 4\pi/3\ \mathring{r}_s$ (or large density). The smaller the parameter $(q^2/n)_c$, the smaller is the value of (q^2/n) which is necessary to achieve a given fissility $X_0 > 3.379$.

Experimentally, to the best of our knowledge, the highest net cluster charges that have so far been reached are about $q = 5$. In any case, a charge of about 24 for a cluster size of about 300, as would be needed for producing Cs bubbles, is probably beyond the present experimental possibilities. Therefore, metals with smaller values of $(q/n)_c$ should be looked for.

On the other hand, developing experimental techniques so as to produce high cluster charges and at the same time larger cluster sizes would also be of great interest concerning the competition between decay by evaporation, by asymmetric, and by symmetric fission [30].

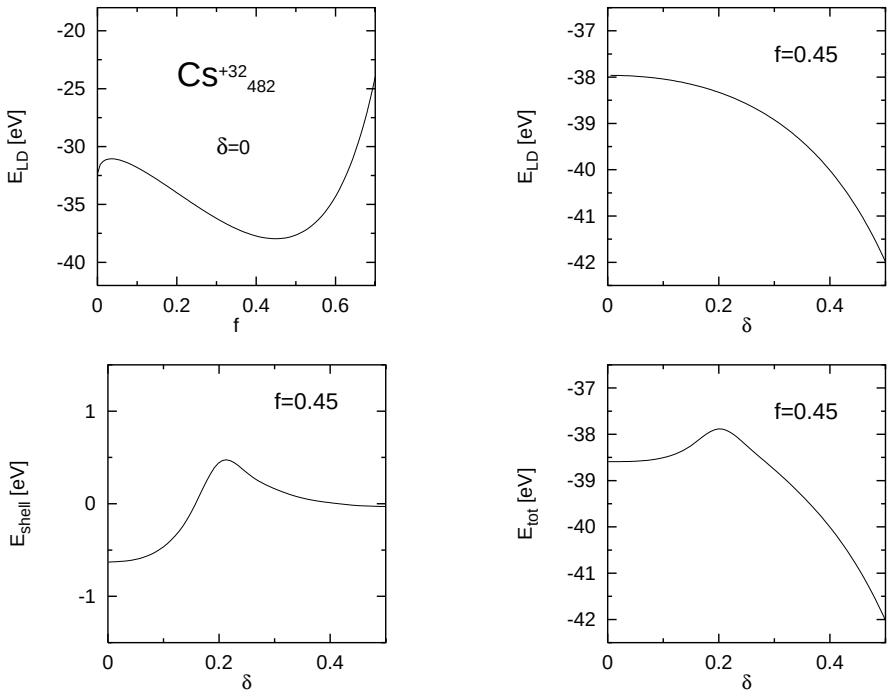

Fig. 9. LD energy of Cs^{+32}_{482} as a function of the hole parameter f (a) and of the deformation δ (b). Figures (c) and (d) represent the shell energy (Eq. (2.16)) and the total energy (Eq. (2.13)) as a function of δ.

4 Summary and discussion

We investigated whether charged metallic clusters may, under certain conditions, find a state of lower energy by forming a spherical bubble rather than a compact sphere. We treated the problem within the simplest possible approximation, *i.e.* jellium model plus a phenomenological shell correction.

As far as the LD-part of the energy is concerned, it could be demonstrated that bubble formation can only occur if the fissility parameter $X_0 > 3.379$. Furthermore, we showed that the shell energy which is obtained for magic numbers of conduction electrons in the bubble-shaped average potential, produces a fission barrier the height of which is of the order of the shell energy for the magic bubble. This barrier protects the bubble from undergoing a (rapid) fission process.

These results were obtained for the example of Cs. For this metal, the number n of Cs atoms and the net charge q necessary for favoring the bubble are quite large ($n \geq 300$, $q \geq 24$). It is probably possible to find other metals, where the conditions can be met more easily. We discussed the criteria for such a search at the end of Section 3.

We did not investigate the importance of decay channels other than symmetric fission, *i.e.* the emission of neutral or weakly charged atoms or molecules. The emission of light charged clusters can be considered as a case of very asymmetric fission. This asymmetric fission surely competes with symmetric fission. We note that symmetric fission is expected to be the preponderant decay channel for highly charged clusters [30]. Checking this theoretical prediction is another reason why it is of great interest to develop experimental techniques to produce highly charged clusters.

Krzysztof Pomorski gratefully acknowledges the warm hospitality extended to him by the Theoretical Physics Group of the Technical University in München as well as the Deutsche Forschung Gemeinshaft for granting a guest professor position which enabled us to perform this research. K. Dietrich is grateful for the hospitality of the Centre d'Études de Bruyères, where a part of the work on the 2nd version of this paper was performed. We also wish to thank Michel Girod for helping us to obtain the results shown in Figures 1 and 2.

References

1. W.D. Knight, K. Clemenger, W.A. de Heer, W.A. Saunders, M.Y. Chou, M.L. Cohen, Phys. Rev. Lett. **52**, 2141 (1984).
2. W.D. Knight, W.A. de Heer, K. Clemenger, W.A. Saunders, Solid State Commun. **53**, 44 (1985).
3. W. Ekardt, Phys. Rev. B **29**, 1558 (1984).
4. D.E. Beck, Solid State Commun. **49**, 381 (1984).
5. M.Y. Chou, A. Cleland, M.L. Cohen, Solid State Commun. **52**, 645 (1984).
6. M. Brack, O. Genzken, K. Hansen, Z. Phys. D **21**, 65 (1991); *ibid.* **19**, 51 (1991).
7. H. Nishioka, K. Hansen, B.R. Mottelson, Phys. Rev. B **42**, 9377 (1990).
8. E. Koch, Phys. Rev. Lett. **76**, 2678 (1996).
9. K. Clemenger, Phys. Rev. B **32**, 1359 (1985).

10. S.M. Reimann, M. Brack, K. Hansen, Z. Phys. D **28**, 235 (1993).
11. S. Frauendorf, V.V. Pashkevich, Z. Phys. D **26**, 98 (1993).
12. I. Hamamoto, B.R. Mottelson, H. Xie, X.Z. Zhang, Z. Phys. D **21**, 163 (1991).
13. V.M. Strutinsky, Sov. J. Nucl. Phys. **3**, 449 (1967); Nucl. Phys. A **95**, 420 (1967); *ibid.* A **122**, 1 (1968).
14. W. Ekardt, Z. Penzar, Phys. Rev. B **38**, 4273 (1988).
15. G. Lauritsch, P.-G. Reinhard, J. Meyer, M. Brack, Phys. Lett. A **160**, 179 (1991).
16. S. Björnholm, J. Borggreen, O. Echt, K. Hansen, J. Pedersen, H.D. Rasmussen, Phys. Rev. Lett. **65**, 1627 (1990); Z. Phys. D **19**, 47 (1991) with references to earlier work.
17. C. Bréchignac, Ph. Cahuzac, F. Carlier, M. de Frutos, J. Ph. Roux, Phys. Rev. B **47**, 2271 (1993), with references to earlier work.
18. C. Bréchignac, H. Busch, Ph. Cahuzac, J. Leygnier, J. Chem. Phys. **101**, 6992 (1994).
19. C. Bréchignac, Ph. Cahuzac, F. Carlier, M. de Frutos, J.Ph. Roux, J. Leygnier, J. Chem. Phys. **102**, 763 (1995).
20. F. Garcias, R.J. Lombard, M. Barranco, J.A. Alonso, J.M. López, Z. Phys. D **33**, 301 (1995).
21. D.H.E. Gross, P.A. Hervieux, Z. Phys. D **35**, 27 (1995); P.A. Hervieux, D.H.E. Gross, Z. Phys. D **33**, 295 (1995); D.H.E. Gross, M.E. Madjet, O. Schapiro, Z. Phys. D **39**, 75 (1997).
22. W.D. Myers, W.J. Swiatecki, Ark. Fys. **36**, 343 (1966); W.D. Myers, W.J. Swiatecki, Nucl. Phys. A **601**, 141 (1996).
23. K. Dietrich, K. Pomorski, Phys. Rev. Lett. **80**, 37 (1998); Nucl. Phys. A **627**, 175 (1997).
24. S. Frank, N. Malinowski, F. Tast, M. Heinebrodt, I.M.L. Billas, T.P. Martin, Z. Phys. D **40**, 250 (1997).
25. S. Springborg, S. Satpathy, N. Malinowski, U. Zimmermann, T.P. Martin, Phys. Rev. Lett. **77**, 1127 (1996).
26. O. Gunnarsson, B.I. Lundquist, Phys. Rev. B **13**, 4274 (1976).
27. S.G. Nilsson, Mat. Fys. Medd. Dan. Vid. Selsk. **29**, 16 (1955).
28. Landolt-Börnstein, *Numerical Data and Functional Relationships in Science and Technology*, Vol. 13, edited by K.-H. Hellwege (Springer Verlag, Berlin-Heidelberg-New York, 1981); S. Flügge, *Electrical Conductivity I*, Handbuch der Physik, Vol. 19 (Springer Verlag, Berlin-Götingen-Heidelberg, 1956).
29. M. Brack, Rev. Mod. Phys. **65**, 677 (1993).
30. U. Näher, S. Björnholm, S. Frauendorf, F. Gracias, C. Guet, Phys. Rep. **285**, 245 (1997).